CANADIAN APPLIED
MATHEMATICS QUARTERLY
Volume 17, Number 2, Summer 2009

MODELLING A RESPIRATORY CENTRAL PATTERN GENERATOR NEURON IN *LYMNAEA STAGNALIS*

SHARENE D. BUNGAY AND SUE ANN CAMPBELL

1 Introduction *Lymnaea stagnalis*, often termed the great pond snail, is characterized in part by its ability to take in oxygen both cutaneously and aerially (via its rudimentary lung). The central nervous system of the *Lymnaea* is composed of a relatively small number of large, identifiable neurons. In 1990, Syed *et al.* [**13**] established that respiratory rhythmogenesis in the *Lymnaea* is controlled by a 3-neuron central pattern generator (CPG) as depicted in Figure 1. Syed *et al.* [**13, 15**] were able to identify and culture the three neurons that make up the CPG, both singly and together, where they reform the same connections as are present *in vivo*. Based on various experimental manipulations, they described the following characteristics of this network. One of these neurons, the RPeD1 (Right Pedal Dorsal 1) neuron, is spontaneously active and is responsible for the initiation of respiration, upon receipt of input from the respiratory orifice. The other two neurons, VD4 (Visceral Dorsal 4) and Ip3I (Input 3), are quiescent except during active respiration. The VD4 neuron (which is responsible for inspiration) is connected via reciprocal inhibitory synaptic connections to both the RPeD1 neuron and the Ip3I neuron (which is responsible for expiration). The Ip3I neuron has excitatory synaptic connections to RPeD1 while the return connections are biphasic, i.e., excitatory via postinhibitory rebound.

The ultimate goal of this work is to develop a mathematical model of the breathing CPG in the *Lymnaea*. The work described here focuses on the development of a Hodgkin-Huxley type mathematical model of the RPeD1 neuron which includes ionic currents for sodium, potassium, and calcium. Results from model simulations are compared to available

This work was supported by Natural Sciences and Engineering Research Council of Canada (NSERC) Discovery Grants to SDB and SAC.

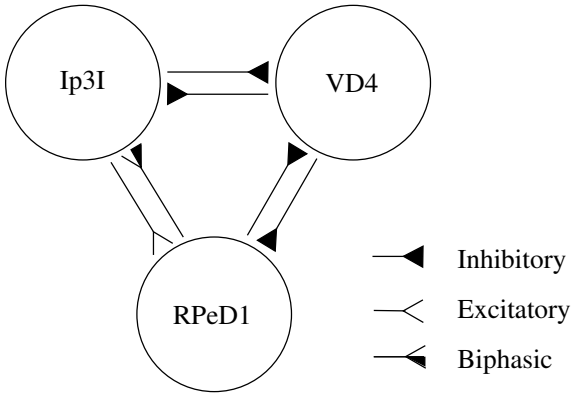

FIGURE 1: Central pattern generator that controls respiration in the *Lymnaea stagnalis*.

experimental data.

2 The model A Hodgkin-Huxley type mathematical model is used to describe the rate of change of membrane potential (V) as

$$C_m \frac{dV}{dt} = -I_{Na} - I_K - I_{Ca} - I_L \tag{1}$$

where C_m is the membrane capacitance, and $I_{Na,K,Ca,L}$ are the total sodium (Na), potassium (K), calcium (Ca), and leak (L) currents respectively. The sodium current I_{Na} is a sum of two currents: a standard sodium current I_{Na_s} and a persistent sodium current I_{Na_p}. Similarly, the potassium current I_K is a sum of two currents: a standard potassium delayed rectifier current I_{KV} and a potassium A current I_A. The individual currents are modelled in the standard way.

$$I_{Na_s} = g_{Na} m^3(V) h(V)(V - V_{Na}), \tag{2}$$

$$I_{Na_p} = g_{Na_p} m_p^3(V) h_p(V)(V - V_{Na}), \tag{3}$$

$$I_A = g_A q^2(V) b(V)(V - V_K), \tag{4}$$

$$I_{KV} = g_{KV} n^4(V)(V - V_K), \tag{5}$$

$$I_{Ca} = g_{Ca} r(V) s(V)(V - V_{Ca}), \tag{6}$$

where $g_z, z \in \{Na, Na_p, A, KV, Ca\}$ are the conductances, and $V_x, x \in \{Na, K, Ca\}$ are the reversal potentials of the currents. The activation variables m, m_p, q, n and r, and inactivation variables h, h_p, b and s, are described by first order equations

$$\frac{dy}{dt} = \frac{y_\infty(V) - y}{\tau_y(V)}, \qquad y \in \{m, m_p, h, h_p, q, b, n, r, s\} \tag{7}$$

where $y_\infty(V)$ denotes the respective steady-state activation/inactivation functions, and $\tau_y(V)$ the time constants of activation/inactivation.

The steady-state activation and inactivation functions are of the form

$$y_\infty(V) = \frac{1}{1 + \exp\left(\frac{V - V_y^{1/2}}{K_y}\right)}, \qquad y \in \{m, m_p, h, h_p, q, b, n, r, s\} \tag{8}$$

where $V_y^{1/2}$ is the half-activation voltage, and K_y is the rate or "slope factor."

The activation time constants are described by the following functions

$$\tau_y(V) = \frac{\tau_{0,y} \exp\left(\frac{\delta_y (V - V_y^{1/2})}{K_y}\right)}{1 + \exp\left(\frac{V - V_y^{1/2}}{K_y}\right)}, \qquad y \in \{m, q, n\} \tag{9}$$

$$\tau_{m_p}(V) = 11.7 + 0.004 \exp\left(\frac{-V}{7.6}\right) \tag{10}$$

$$\tau_r(V) = t_r, \tag{11}$$

where t_r is a constant. The inactivation time constants were taken to be voltage independent, i.e., constant:

$$\tau_y(V) = t_y, \qquad y \in \{h, h_p, b, s\}.$$

Values for all other parameters of the model were obtained either directly from the literature or via fitting of experimental data found in the literature. The values so obtained, and the sources, are given in Table 1. The membrane capacitance was taken to be $C_m = 0.333$ μF in accordance with data from [**7**].

z	y	g_z μS	V_z mV	$V_y^{1/2}$ mV	K_y mV	$\tau_{0,y}$ ms	δ_y	t_y ms
Na[1]	m	0.5	22	-34.74	-9.32	6.98	0.16	
	h			-59.95	9.4			3.44
Na_p[2]	m_p	0.25	22	-18	-16.4			
	h_p			-46	7.43			300
Ca[3]	r	0.05	80	-18.08	-7.2			10.5
	s			-24	8.7			90
KV[4]	n	0.2	-70	-42.5	-24.5	62.56	0.83	
A[4]	q	0.01	-70	-62.3	-8.3	16.1	0.087	
	b			-69.1	8.8			200
L[5]		0.00025	-12.2					

[1] Parameter values computed using data from [**9**] and [**4**].
[2] Parameter values computed using data from [**8**].
[3] Parameter values computed using data from [**12**] and [**10**].
[4] Parameter values computed using data from [**11**].
[5] Parameter values set so that the resting potential would be in the physiological range given in [**7**].

TABLE 1: Parameter values used.

3 Results Numerical simulations of the model were carried out using XPPAUT, a differential equation simulation tool developed by B. Ermentrout. See [**3**] for details. A Runge-Kutta fourth order solver with stepsize 0.1 ms was used. Figure 2 illustrates the spontaneous spiking behaviour of the model with the parameter values listed in Table 1. While the frequency of the spiking, ≈ 0.65 Hz, is consistent with experimental observations [**7**], the spike amplitude is smaller than that seen in experiments. Examination of the individual currents indicate that sodium initiates the spiking behaviour, after which calcium takes over. The potassium current is involved in the repolarization phase, with I_A causing the shoulder of the action potential.

To determine the robustness of spiking in the model with respect to the conductances, we carried out numerical bifurcation studies varying each conductance separately. These studies were done using the AUTO numerical continuation package [**2**] within the XPPAUT package. One such study, using g_{Na} as the bifurcation parameter, is shown in Figure 3. In this example, stable oscillations exist between two limit points at $g_{Na} = 0.4946$ and 1.004. The unstable oscillations created by the limit

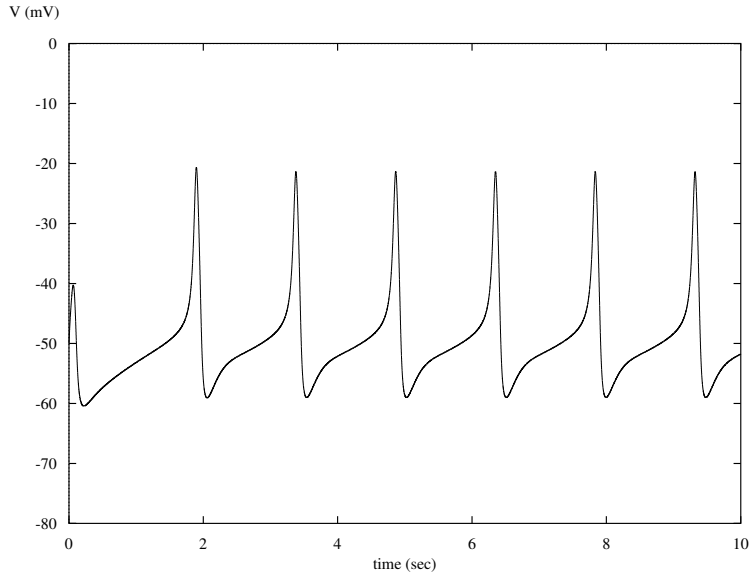

FIGURE 2: Spontaneous spiking behaviour exhibited by a Hodgkin-Huxley like model of the RPeD1 neuron. Initial conditions: $V = -50$, $m = m_p = n = q = r = 0$, $h = h_p = b = s = 1$.

points are lost in subcritical Hopf bifurcations. A similar sequence of bifurcations occurred for all the conductances. A summary of all the numerical bifurcation studies is given in Table 3.

We also considered the situation where a constant applied current is included in the voltage equation:

$$C_m \frac{dV}{dt} = -I_{Na} - I_K - I_{Ca} - I_L + I_{\text{applied}} \tag{12}$$

representing external input to the neuron. When the applied current is varied, we observe the same bifurcation sequence as found for g_{Ca}. Stable oscillations exist for I_{applied} between -0.0024 μA (a limit point) and 0.1533 μA (a supercritical Hopf bifurcation). In this range of I_{applied} the period of the oscillations decreases from 4168 ms to 180 ms.

4 Discussion and conclusions We have created a Hodgkin-Huxley type model for the RPeD1 neuron of the freshwater pond snail,

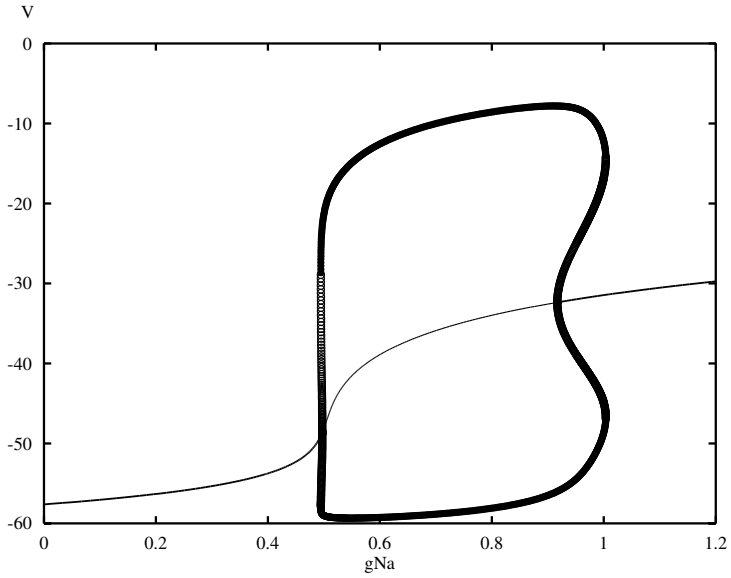

FIGURE 3: Numerical bifurcation curves for g_{Na}. Thick/thin lines correspond to stable/unstable equilibrium points, filled/open circles correspond to stable/unstable periodic orbits. Stable oscillations occur for $g_{Na} \in [0.4946, 1.004]$.

including 5 different ionic currents. Model results demonstrate spontaneous realistic spiking behaviour with a frequency that matches experimental results. Using numerical bifurcation analysis we established bounds on the values of the conductances and the value of the applied current for the model to exhibit periodic behaviour. Within these bounds, the frequency of the oscillations varies from 0.24 Hz to 7.75 Hz.

The bifurcation analysis is useful from a modelling standpoint, as it establishes how robust the spiking behaviour is to variations in the parameters. From Table 2, one can see that the model behaviour is quite robust with respect to changes in the sodium conductances (g_{Na}, g_{Na_p}), but less so with respect to changes in the calcium and delayed rectifier potassium conductances (g_{Ca}, g_{KV}). The model is particularly sensitive to changes in the potassium A current conductance (g_A).

As discussed in the introduction, *Lymnaea stagnalis* does not breathe continuously through its lungs, but alternates between cutaneous respiration while the animal is submerged and aerial respiration when it

Parameter	Bifurcation type	Value (μS)	Period (ms)	Stable Oscillations
g_{Na}	subcritical Hopf	0.4972	1450	[0.4946, 1.004]
	limit point	0.4946	2103	
	limit point	1.004	238	
	subcritical Hopf	0.9171	175	
g_{Na_p}	subcritical Hopf	0.2471	1477	[0, 0.2446]
	limit point	0.2446	2175	
g_{Ca}	subcritical Hopf	0.0498	1468	[0.04967, 0.1339]
	limit point	0.04967	2146	
	supercritical Hopf	0.1339	129	
g_A	subcritical Hopf	0.01022	1541	[0, 0.01042]
	limit point	0.01042	2345	
g_{KV}	subcritical Hopf	0.1351	190	[0.1347, 0.2007]
	limit point	0.1347	193	
	limit point	0.2007	2128	
	subcritical Hopf	0.2004	1458	

TABLE 2: Location and type of bifurcation points for each conductance.

surfaces. How often the animal surfaces to breathe and the frequency of its breathing at the surface depend on the amount of oxygen present in the water, with more frequent breathing corresponding to lower oxygen levels [**14**]. Experimental evidence [**1**] indicates that the regulation of the breathing frequency is due to an excitatory input from an oxygen sensing periphery neuron to the RPeD1 neuron. The increase in the frequency of the spontaneous oscillations in our model RPeD1 neuron as the applied current is increased suggests a mechanism for this observation: increase of the intrinsic RPeD1 oscillation frequency leads to increase of the CPG network frequency which in turn leads to an increase in breathing frequency. Clearly this needs further investigation in a model for the full CPG network. Finally, we note that a small negative applied current eliminates the oscillations in our model RPeD1 neuron. This is consistent with experimental observations that inhibitory input from periphery neurons [**5**] or other interneurons [**6**] can suppress the oscillations of the RPeD1 neuron.

REFERENCES

1. H. J. Bell, T. Inoue and N. I. Syed, *A peripheral oxygen sensor provides direct activation of an identified respiratory CPG neuron in* Lymnaea, in: M. J. Poulin and R. J. A. Wilson (eds.), Advances in Experimental Medicine and Biology, Springer, New York, 2008.
2. E. J. Doedel and J. P. Kernevez, *Auto: Software for Continuation Problems in Ordinary Differential Equations*, Applied Mathematics Rep., California Institute of Technology, 1986.
3. G. B. Ermentrout, *Similating, Analyzing and Animating Dynamical Systems: A Guide to XPPAUT for Researcher and Students*, SIAM, Philadelphia, PA, 2002.
4. J. Györi, O. Platoshyn, D. O. Carpenter and J. Salánki, *Effect of inorganic and organic tin compounds on ACh- and voltage-activated Na currents*, Cell. Mol. Neurobiol. **20** (2000), 591–604.
5. T. Inoue, Z. Haque, K. Lukowiak and N. I. Syed, *Hypoxia-induced respiratory patterned activity in* Lymnaea *originates in the periphery*, J. Neurophysiology, **86** (2001), 156–163.
6. T. Inoue, M. Takasaki, K. Lukowiak and N. I. Syed, *Inhibition of the respiratory pattern-generating neurons by an identified whole-body withdrawal interneuron of* Lymnaea, J. Experimental Biol. **199** (1996), 1887–1898.
7. C. McComb, R. Meems, N. Syed and K. Lukowiak, *Electrophysiologial differences in the CPG aerial respiratory behaviour between juvenile and adult* Lymnaea, J. Neurophysiol. **90** (2003), 983–992.
8. E. S. Nikitin, T. Kiss, K. Staras, M. O'Shea, P. R. Benjamin and G. Kemenes, *Persistent sodium current is a target for cAMP-induced neuronal plasticity in a state-setting modulatory interneuron*, J. Neurophysiol. **95** (2006), 453–463.
9. S. Onizuka, T. Kasaba, T. Hamakawa, S. Ibusuki and M. Takasaki, *Lidocaine increases intracellular sodium concentration through voltage-dependent sodium channels in an identified* Lymnaea *neuron*, Anesthesiology **101** (2004), 110–119.
10. S. Onizuka, T. Kasaba, T. Hamakawa and M. Takasaki, *Lidocaine excites both pre- and postsynaptic neurons of reconstructed respiratory pattern generator in* Lymnaea stagnalis, Anesth. Analg. **100** (2005), 175–182.
11. M. Sakakibara, F. Okuda, K. Nomura, K. Watanabe, H. Meng, T. Horikoshi and K. Lukowiak, *Potassium currents in isolated statocyst neurons and RPeD1 in the pond snail,* Lymnaea stagnalis, J. Neurophysiol. **94** (2005), 3884–3892.
12. K. Staras, J. Györi and G. Kemenes, *Voltage-gated ionic currents in an identified modulatory cell type controlling molluscan feeding*, European J. Neuroscience **15** (2002), 109–119.
13. N. I. Syed, A. G. M. Bulloch and K. Lukowiak, *In vitro reconstruction of the respiratory central pattern generator of the mollusk* Lymnaea, Science **250** (1990), 282–285.
14. N. I. Syed, D. Harrison and W. Winlow, *Respiratory behaviour in the pond snail* Lymnaea stagnalis. *I. Behavioural analysis and the identification of motor neurons*, J. Comparative Physiology A, **169** (1991), 541–555.
15. N. I. Syed, H. Zaidi and P. Lovell, In vitro *reconstruction of neuronal networks: a simple model systems approach*, in: U. Windhurst and H. Johansson (eds.), Modern Techniques in Neuroscience Research, 361–377, Springer, Berlin, 1999.

Corresponding author: Sharene D. Bungay
Department of Computer Science,
Memorial University of Newfoundland,
St. John's, NL, A1B 3X5.
E-mail address: sharene@mun.ca

Department of Applied Mathematics,
University of Waterloo, Waterloo, ON, N2L 3G1.
E-mail address: sacampbell@uwaterloo.ca